Neutral glycosphingolipids in human blood: a precise mass spectrometry analysis with special reference to lipoprotein-associated Shiga toxin receptors[S]

Christian H. Schweppe,[1,*] Petra Hoffmann,[1,*] Jerzy-Roch Nofer,[†] Gottfried Pohlentz,[§] Michael Mormann,[§] Helge Karch,[*] Alexander W. Friedrich,[*,] and Johannes Müthing[2,*,**]**

Institute for Hygiene,[*] Institute for Clinical Chemistry and Laboratory Medicine,[†] and Institute for Medical Physics and Biophysics,[§] University of Münster, D-48149 Münster, Germany; and Interdisciplinary Center for Clinical Research (IZKF) Münster,[**] D-48149 Münster, Germany

Abstract **Shiga toxin (Stx)-producing *Escherichia coli* are the leading cause of hemorrhagic colitis and life-threatening extraintestinal complications in humans. Stx1 and Stx2 are transferred by yet to be delineated mechanisms from the intestine to the circulation where they injure microvascular endothelial cells. The resulting vascular lesions cause renal failure and brain damage. Because lipoproteins are potential carriers of Stx through the circulation, we investigated human lipoprotein-associated neutral glycosphingolipids (GSLs) with emphasis on high (globotriaosylceramide) and low (globotetraosylceramide) affinity Stx-receptors. TLC overlay employing Stx1, Stx2, and anti-GSL antibodies demonstrated preferential distribution of globo-series GSLs to very low- and low-density lipoproteins compared with minor association with high-density lipoproteins. Electrospray ionization quadrupole time-of-flight mass spectrometry portrayed C24:0/C24:1 and C16:0 as the major fatty acid of the ceramide moieties of Stx-receptors carrying nonvarying d18:1 sphingosine. This structural heterogeneity was also found in precursor lactosylceramide, glucosylceramide, and galactosylceramide, the last showing an exceptionally high degree of hydroxylated C24 fatty acids. Our findings provide the basis for exploring the functional role of lipoprotein-associated Stx-receptors in human blood.**—Schweppe, C. H., P. Hoffmann, J-R. Nofer, G. Pohlentz, M. Mormann, H. Karch, A. W. Friedrich, and J. Müthing. **Neutral glycosphingolipids in human blood: a precise mass spectrometry analysis with special reference to lipoprotein-associated Shiga toxin receptors.** ***J. Lipid Res.*** **2010.** 51: **2282–2294.**

Supplementary key words monohexosylceramides • glycolipids • galactosylceramide • glucosylceramide • globotriaosylceramide

Glycosphingolipids (GSLs) are amphipathic molecules that contain a hydrophilic oligosaccharide residue and a hydrophobic ceramide moiety (1, 2). The ceramide consists of a sphingoid base that is linked with a fatty acid via N-acylation forming the lipid anchor of GSLs. Much effort is currently spent to analyze the biodiversity of sphingolipid structure, metabolism, and function (3, 4). Neutral GSLs as well as sialic acid carrying gangliosides are most prominently located in the outer leaflet of the plasma membrane of animal cells where they are clustered in lipid rafts (5, 6), but recent studies have also pointed to important functional roles in the nucleus (7). Their oligosaccharides protrude from the cell surface rendering GSLs candidates for cell-cell interactions (8), particularly in the development and pathogenesis of organs (9, 10). Furthermore, GSLs play important biological roles in the pathophysiology of many infections and serve as receptors for bacteria (11) and bacterial toxins, including Shiga toxins (Stxs) (12, 13).

Stxs are AB_5 holotoxins, which have been divided into two families, Stx1 and Stx2, each of which consists of the major Stx type and several variants (14, 15). The pentameric B-subunit of Stx1 binds to globotriaosylceramide (Gb3Cer/CD77) (16) on the surface of susceptible

This work was supported by grants from the "Deutsche Forschungsgemeinschaft" (DFG)-funded International Graduate School "Molecular Interactions of Pathogens with Biotic and Abiotic Surfaces" (GRK 1409, collaboration between the projects 3.10 of J.M. and 3.6 of H.K.), cooperative projects MU845/4-1 (J.M.) and FR2569/1-1 (A.W.F.), and the Interdisciplinary Center for Clinical Research (IZKF) Münster project no. Müth2/028/10.

Manuscript received 10 March 2010 and in revised form 5 May 2010.

Published, JLR Papers in Press, 5 May 2010
DOI 10.1194/jlr.006759

Abbreviations: CID, collision-induced-dissociation; ESI Q-TOF-MS, electrospray ionization quadrupole time-of-flight mass spectrometry; GalCer, galactosylceramide; Gb3Cer, globotriaosylceramide; Gb4Cer, globotetraosylceramide; Gg3Cer, gangliotriaosylceramide; Gg4Cer, gangliotetraosylceramide; GlcCer, glucosylceramide; GSL, glycosphingolipid; HUS, hemolytic uremic syndrome; Lc2Cer, lactosylceramide; MHC, monohexosylceramide; nLc4Cer, neolactotetraosylceramide; STEC, Stx-producing *Escherichia coli*; Stx, Shiga toxin.

[1] C. H. Schweppe and P. Hoffmann contributed equally to the publication.

[2] To whom correspondence should be addressed.
e-mail: jm@uni-muenster.de

[S] The online version of this article (available at http://www.jlr.org) contains supplementary data in the form of one table and two figures.

endothelial cells (17). Stxs are internalized and undergo retrograde transport through the Golgi apparatus to the endoplasmic reticulum (18). After translocation into the cytosol, the enzymatically active A1 fragment exerts its toxic function due to specific depurination of adenosine at a highly conserved loop of the 60S rRNA, causing death of the target cell through inhibition of protein synthesis (19, 20). Vascular damage caused by Stx-producing *Escherichia coli* (STEC), the major causes of hemorrhagic colitis and the life-threatening hemolytic uremic syndrome (HUS), is largely mediated by Stxs, which particularly injure endothelial cells in the kidney, the brain, and other organs and also participate in thrombotic mechanisms (15, 17, 21–23). After being released by the infecting STEC in the intestine, Stx is translocated across the gut into circulation (24) and transported to endothelial cells. Importantly, Gb3Cer has not been detected in human gastroepithelial cells (25), and the mechanism of toxin translocation across the intestinal barrier remains an enigma. Although the role of polymorphonuclear leukocytes as a Stx carrier has been indicated (26, 27), the mechanism of toxin delivery is still a matter of debate. Interestingly, lipoproteins can bind GSLs, including Gb3Cer (28), and it seems possible that Stx could be cotransported, bound in a piggyback fashion with dietary lipoproteins, from the lumen of the intestine to the circulation (29). However, knowledge about the structural diversity of GSLs in lipoproteins is rather poor and little is known about their functional role in human blood. Though the existence of neutral GSLs in lipoproteins is well known (30, 31), the composition of GSLs, being minor constituents of lipoproteins, and their fine structure have generally drawn little attention (32, 33). This prompted us to perform a compositional analysis of neutral GSLs in human blood with special reference to monohexosylceramides and Stx receptors and their association with lipoproteins. Notably, glucosylceramide (GlcCer) has been reported to modulate the Stx-mediated cytotoxic effect (34) and may directly contribute to venous thrombosis (35), and galactosylceramide (GalCer) has been identified as a (co)receptor of type 1 human immunodeficiency virus (36, 37).

Initially we started with TLC overlay detection of the globo-series GSLs Gb3Cer and globotetraosylceramide (Gb4Cer) and the precursor GSLs monohexosylceramide and lactosylceramide (Lc2Cer) using anti-GSL specific antibodies as well as Stx1 and Stx2 for the identification of neutral GSLs isolated from human plasma. We then characterized the TLC detected neutral GSLs by MS employing MS^1 and tandem MS^2, which has not been reported before. Their specific localization was then determined in lipoprotein fractions of different densities, which were prepared from the same batch of human plasma used for the combined TLC-MS analysis. Our findings provide the basis for further exploring the functional role of neutral GSLs in STEC infections and support the hypothesis that lipoprotein-associated GSLs may interact with Stxs in the gut and/or human blood.

MATERIALS AND METHODS

Human plasma

Frozen pooled fresh plasma of healthy donors of blood group A was obtained from the Heart and Diabetes Centre Northrhine-Westphalia (Bad Oeynhausen, Germany; charge 0426 127710 1). The plasma (protein concentration 69.4 mg/ml) was thawed, filtrated through a sterile filter (pore size 0.2 μm), and aliquots of 360 ml and 100 ml were immediately used for the preparation of lipoproteins and the extraction of GSLs, respectively (see below).

Preparation of lipoprotein fractions from human plasma

VLDL (fraction I, d = 0.94 to 1.006 g/ml), LDL (fraction II, d = 1.019 to 1.063 g/ml), and HDL (fraction III, d = 1.125 to 1.210 g/ml) were isolated from 360 ml of human plasma by discontinuous KBr gradients as described by Havel et al. (38). Fraction I comprises chylomicrons, is enriched in VLDL, and contains in addition intermediate-density lipoproteins (IDL), thereafter named "VLDL". Due to their high content of LDLs and HDLs, fractions II and III were designated as "LDL" and "HDL", respectively. The lipoprotein fractions were dialyzed against 0.3 mmol/l Tris-HCl, 0.14 mol/l NaCl, 1.0 mmol/l EDTA, pH 7.2, and stored under exclusion of light at 4°C for no longer than 7 days. The protein concentration in lipoprotein fractions [VLDL (1.3 mg/ml), LDL (6.4 mg/ml), and HDL (11.4 mg/ml)] were determined by the method of Lowry et al. (39).

Isolation and purification of neutral GSLs from human plasma

One hundred milliliters of pooled plasma were dialyzed against deionized water followed by lyophilization. The residue was extracted twice with chloroform/methanol/water (30/60/8, each by vol.). After rotary evaporation, the extract was resolved in 100 ml of aqueous 1 N NaOH and incubated for 2 h at 37°C in order to saponify coextracted phospholipids and triacylglycerides. After neutralization with 10 N HCl followed by dialysis and lyophilization, neutral GSLs were separated from gangliosides by anion-exchange column chromatogrpahy employing DEAE-Sepharose CL-6B (GE Healthcare, München, Germany) in the acetate form and subsequently purified by silica gel 60 (particle size 0.040 to 0.063 mm, Merck, Darmstadt, Germany) chromatography according to standard procedures (40–42). The neutral GSL fraction was adjusted to 2 ml of chloroform/methanol (2/1, v/v) whereby 1 μl corresponds to 50 μl of plasma (equivalent to 3.47 mg of plasma protein).

Isolation of GSLs from lipoprotein preparations

Three types of lipoprotein fractions were prepared according to their density (see "Preparation of lipoprotein fractions from human plasma"). Aliquots of VLDL, corresponding to 4 mg of lipoprotein, and aliquots of LDL and HDL, equivalent to 20 mg of lipoprotein, respectively, were dialyzed against deionized water and dried by rotary evaporation. After saponification of nonGSL contaminants with 1 N NaOH for 1 h at 37°C and neutralization with 10 N HCl, samples were lyophilized. GSLs were extracted from the residues with chloroform/methanol/water (30/60/8, v/v/v) under sonication. The extracts were centrifuged and the supernatants dried by rotary evaporation. The residues were redissolved in chloroform/methanol (2/1, v/v) and adjusted to concentrations whereby 1 μl of extract corresponds to 1 μg of lipoprotein.

Stx1 and Stx2

Stx1 and Stx2 were purified from *E. coli* C600(H19J) carrying the stx_1 gene from *E. coli* O26:H11 strain H19 (43) and from *E. coli*

C600(933W) carrying the *stx*$_2$ gene from *E. coli* O157:H7 strain EDL933 (44), respectively. Briefly, bacteria were disintegrated by sonication and subjected to extraction with polymyxin B (3000 U/ml) (Sigma-Aldrich Chemie GmbH, Taufkirchen, Germany). After centrifugation, the supernatant containing crude Stx was concentrated by ultrafiltration and subjected to chromatography on hydroxylapatite column followed by chromatofocusing (45, 46). The column fractions containing Stx were pooled, dialyzed, and aliquots were stored at −70°C until use. Purity of the Stx1 and Stx2 preparations was monitored by SDS-PAGE, and the structural integrity of both toxins was checked by peptide mapping employing MS (13).

Anti-GSL, anti-Stx1, and anti-Stx2 antibodies

All polyclonal rabbit and chicken antibodies were produced according to the method of Kasai et al. (47). The preparation and specificities of the antibodies against various neutral GSLs have been reported in previous publications. Structures of GSLs and the antibody-relevant references are listed in **Table 1**. Mouse IgG monoclonal antibodies 109/4-E9b and 135/6-B9 (Sifin, Berlin, Germany) were used for the detection of Stx1 and Stx2, respectively.

Reference GSLs

The nomenclature of GSLs follows the IUPAC-IUB recommendations (48). All monosaccharides are in D-configuration and all glycosidic linkages originate from the C1 hydroxyl group. A GlcCer fraction from human Gaucher's spleen was purchased from Sigma-Aldrich (G-9884; St. Louis, MO) and found being mostly composed of GlcCer (d18:1, C24:1/C24:0), GlcCer (d18:1, C22:0), and GlcCer (d18:1, C16:0). A GalCer fraction was prepared from human brain according to standard procedures (40, 49) harboring GalCer (d18:1, C24:1), GalCer (d18:1, h24:1/h24:0), and GalCer (d18:1, C18:0) as the major constituents. Neutral GSL reference mixture 1 comprising Lc2Cer, Gb3Cer, and Gb4Cer as the major constituents was isolated from human erythrocytes as previously described (50). Ten micrograms of mixture 1 contained 0.3 μg and 0.6 μg of Lc2Cer (d18:1, C24:1/C24:0) and Lc2Cer (d18:1, C16:0), respectively, 1.7 μg and 0.4 μg of Gb3Cer (d18:1, C24:1/C24:0) and Gb3Cer (d18:1, C16:0), respectively, and 5.7 μg and 0.1 μg of Gb4Cer (d18:1, C24:1/C24:0) and Gb4Cer (d18:1, C16:0), respectively, as well as some minor, not further identified neutral GSLs. Neutral GSL reference mixture 2 containing Lc2Cer and nLc4Cer as the major compounds (51) was prepared from human granulocytes. Ten micrograms of mixture 2 contained 1.9 μg and 2.6 μg of Lc2Cer (d18:1, C24:1/C24:0) and Lc2Cer (d18:1, C16:0), respectively, and 3.5 μg and 2.0 μg of nLc4Cer (d18:1, C24:1/C24:0) and nLc4Cer (d18:1, C16:0), respectively. Individual neutral GSLs of the reference mixtures were quantified as pinkish-violet orcinol stained bands with a CD60 scanner (Desaga, Heidelberg, Germany, software ProQuant®, version 1.06.000) in reflectance mode at λ=544 nm with a light beam slit of 0.02 mm × 3 mm.

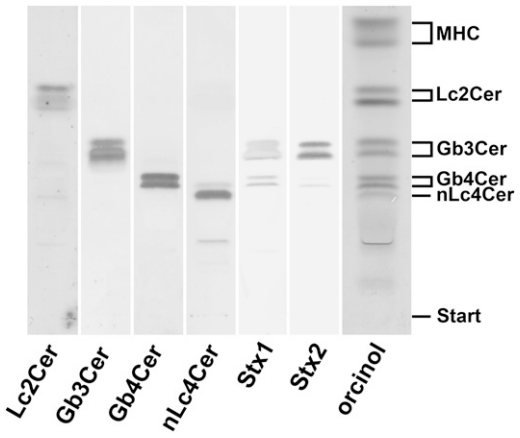

Fig. 1. TLC immunodetection of individual GSLs in the neutral GSL preparation of human plasma. Amounts of GSLs applied for the orcinol stain correspond to 34.7 mg and those for the TLC overlay assays using anti-GSL antibodies as well as Stx1 and Stx2 are equivalent to 17.4 mg of human plasma proteins. Bound anti-GSL antibodies specific for Lc2Cer, Gb3Cer, Gb4Cer, and nLc4Cer as well as Stx1/anti-Stx1-antibody and Stx2/anti-Stx2-antibody were visualized with alkaline phosphatase conjugated secondary antibodies and BCIP as a substrate. The vertical white lines indicate areas of noncontiguous lanes assembled. The GSL structures and backgound information on the employed antibodies and Stxs are provided in Table 1. MHC, monohexosylceramides.

High-performance TLC

Neutral GSLs were separated on glass-backed silica gel 60 precoated high-performance TLC plates (no. 1.05633.0001; Merck) in the solvent chloroform/methanol/water (120/70/17, each by vol., with 2 mM $CaCl_2$). The monohexosylceramides GlcCer and GalCer were separated as borate complexes (52). Briefly, the plate was loaded with the sample and exhaustively sprayed with 1.5% (w/v) aqueous $Na_2B_4O_7$ solution. After careful drying, GSLs were separated in alkaline solvent composed of chloroform/methanol/water/32% NH_4OH (65/25/4/0.5, each by vol.). For preparative purposes, GSLs were stained with primulin (Sigma; P-7522) (53) and extracted from the silica gel as previously described (54).

TLC immunostaining

The TLC immunodetection procedure using anti-GSL antibodies and Gb3Cer-binding Stx1 and Stx2 in conjunction with anti-Stx1 and anti-Stx2 antibodies, respectively, was employed as previously described (50, 55–59). All primary anti-GSL and alkaline phosphatase-labeled secondary antibodies (Dianova, Hamburg, Germany) were overlayed to the TLC plate in 1:2000 dilutions. Bound secondary antibodies were visualized by color development using 5-bromo-4-chloro-3-indolyl phosphate *p*-toluidine salt (BCIP; Biomol, Hamburg, Germany).

Extraction of GSLs from silica gel of TLC plates

The silica gel of primulin-, antibody-, and Stx-detected GSL bands was extracted with chloroform/methanol/water (30/60/8,

TABLE 1. Monoclonal antibodies, polyclonal antibodies, Stx1, and Stx2 employed for the identification and structural characterization of neutral GSLs from human plasma

GSL	Structure	References
Antibodies		
Lc2Cer	Galβ4Glcβ1Cer	51, 56
Gb3Cer	Galα4Galβ4Glcβ1Cer	50, 51, 56
Gb4Cer	GalNAcβ3Galα4Galβ4Glcβ1Cer	50, 56
Gg3Cer	GalNAcβ4Galβ4Glcβ1Cer	50, 51, 56
Gg4Cer	Galß3GalNAcβ4Galβ4Glcβ1Cer	51, 56
nLc4Cer	Galβ4GlcNAcβ3Galβ4Glcβ1Cer	51, 55, 56
Stx1 and Stx2		
Gb3Cer	Galα4Galβ4Glcβ1Cer	13, 50, 57-59
Gb4Cer	GalNAcβ3Galα4Galβ4Glcβ1Cer	13, 50, 57-59

The listed antibodies are polyclonal chicken IgY antibodies with the exception of anti-Gg3Cer (2D4, mouse monoclonal IgM) and anti-Gg4Cer antibody (rabbit polyclonal IgG). The nomenclature of GSLs follows the IUPAC-IUB recommendations 1997 (48). Stx1 and Stx2 pereferentially bind to Gb3Cer and, to a minute extent, to Gb4Cer as shown in the cited references. References represent examples for antibody and Stx specificity analyses and refer to some applications.

each by vol.) under sonication (54). The supernatants from 3-fold extractions were pooled, dried, redissolved in methanol, and analyzed by MS without further purification.

ESI Q-TOF-MS

The extracted GSL samples were analyzed in positive ion mode by electrospray ionization quadrupole time-of-flight mass spectrometry (ESI Q-TOF-MS^1) and low-energy collision-induced-dissociation (CID) MS^2 using a Q-TOF mass spectrometer (Micromass, Manchester, UK). After selecting the precursor ions of interest with the first quadrupole, CID was performed to obtain fragment ions enabling sequence analysis [for further details see Meisen et al. (54, 60) and Schweppe et al. (58)]. The nomenclature introduced by Domon and Costello (61, 62) and Adams and Ann (63) was used for the assignment of the fragment ions.

RESULTS

TLC immunodetection of human plasma neutral GSLs

The initial identification of neutral GSL structures, deduced from their chromatographic behavior in comparison to reference neutral GSLs, demonstrated monohexosylceramide(s), Lc2Cer, and the globo-series neutral GSLs Gb3Cer and Gb4Cer (subsequently confirmed by TLC immunostaining with specific antibodies) as the predominant GSLs in human plasma as shown in the orcinol stain of **Fig. 1**. TLC scanning of the prevalent orcinol-stained neutral GSL bands on a percentage level revealed an almost equal ratio of high abundant monohexosylceramides and Lc2Cer (31% and 30%, respectively) and a high content of Gb3Cer and Gb4Cer (18% and 16%, respectively) compared with rather low amounts of nLc4Cer (5%) (see supplementary Table I). The preliminarily identified neutral GSLs were then confirmed by means of TLC immunostaining using specific anti-GSL antibodies, Stx1/anti-Stx1 and Stx2/anti-Stx2, which are listed in **Table 1** along with the detected GSL structures. All GSLs appeared as double bands in the orcinol stain as well as in the overlay assays, suggesting fatty acid heterogeneity in the lipid ceramide anchor. Stx1 and Stx2 showed strong binding toward Gb3Cer and only minor interaction with Gb4Cer as shown

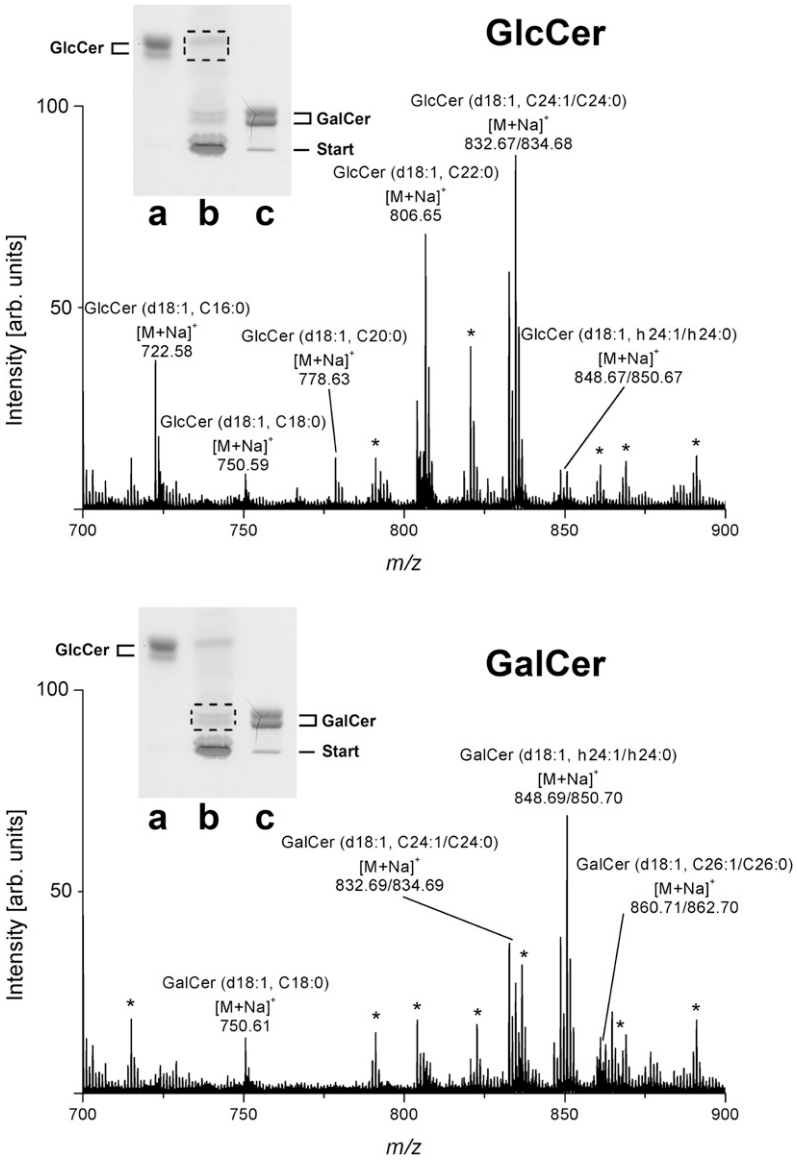

Fig. 2. ESI Q-TOF-MS^1 spectra of GlcCer and GalCer from human plasma. The spectra were prepared from silica gel extracts of primulin-stained monohexosylceramides after TLC separation as borate complexes in alkaline solvent. MS^1 spectra of GlcCer (upper panel) and GalCer (lower panel) were recorded in the positive ion mode. Dotted frames in the insets, which show the orcinol stain of a TLC plate, indicate the silica gel positions from which primulin-detected GlcCer and GalCer were extracted, respectively. Lane a: Reference GlcCer, 7 μg; lane b: neutral GSL mixture corresponding to 34.7 mg of human plasma protein; lane c: reference GalCer, 10 μg. Unassigned ion species, which originate most likely from coextracted lipids are marked with asterisks and were not further analyzed. Major [M+Na]$^+$ ions of monohexosylceramides and their proposed structures are listed in Table 2.

in the TLC binding assay of Fig. 1. The ganglio-series neutral GSLs Gg3Cer and Gg4Cer were not detected in the neutral GSL fraction of human plasma (data not shown).

Monohexosylceramides

The monohexosylceramides were separated as borate complexes in alkaline solvent into GlcCer and GalCer in comparison to reference GlcCer from human Gaucher's spleen and GalCer from human brain, respectively (see insets of **Fig. 2**). The relative amount of GlcCer and GalCer was determined by TLC scanning of orcinol-stained bands to be 53% and 47%, respectively. Further detailed structural characterization was performed by ESI Q-TOF-MS after preparative TLC. For this purpose, the silica gel of primulin stained bands was scraped off the plate, extracted with an approximate recovery rate of 80%, and the GSLs in the extracts analyzed by MS in the positive ion mode. The monosodiated ions obtained by ESI Q-TOF-MS^1 (Fig. 2, upper panel) resulted in the identification of GlcCer (d18:1, C24:1/C24:0), GlcCer (d18:1, C22:0), and GlcCer (d18:1, C16:0) as the most prominent GlcCer species, accompanied by minor GlcCer variants carrying C18:0, C20:0, and hydroxylated C24:1 (h24:1) and C24:0 (h24:0) fatty acids (**Table 2**). MS^1 analysis of the GalCer double band (Fig. 2, lower panel) demonstrated hydroxylated GalCer (d18:1, h24:1/h24:0) and nonhydroxylated GalCer (d18:1, C24:1/C24:0) as the major GalCer species (Table 2). Less abundant $[M+Na]^+$ ions were indicative for GalCer (d18:1, C18:0) and GalCer (d18:1, C26:1/C26:0).

The proposed structures, and particularly the assessment of hydroxylated species of GlcCer and GalCer, were further verified by MS^2 analysis. The MS^2 spectrum, together with the corresponding fragmentation scheme of GalCer (d18:1, h24:0), is shown as a representative example of a hydroxylated monohexosylceramide in **Fig. 3**. The fragment ions obtained by internal cleavage of the ceramide portion clearly evidenced the occurrence of h24:0 and the concomitant appearance of sphingosine (d18:1) as indicated by specific diagnostic ions.

TABLE 2. Major monosodiated ions of monohexosylceramides from human plasma identified by ESI Q-TOF-MS and their proposed structures

$[M+Na]^+$ *m/z* (Calculated)	$[M+Na]^+$ *m/z* (Experimental)	Proposed Structure
722.55	**722.58**	**GlcCer (d18:1, C16:0)**
750.59	750.59	GlcCer (d18:1, C18:0)
778.62	778.63	GlcCer (d18:1, C20:0)
806.65	**806.65**	**GlcCer (d18:1, C22:0)**
832.66	**832.67**	**GlcCer (d18:1, C24:1)**
834.68	**834.68**	**GlcCer (d18:1, C24:0)**
848.66	848.67	GlcCer (d18:1, h24:1)
850.68	850.67	GlcCer (d18:1, h24:0)
750.59	750.61	GalCer (d18:1, C18:0)
	750.61	
832.66	**832.69**	**GalCer (d18:1, C24:1)**
834.68	**834.69**	**GalCer (d18:1, C24:0)**
848.66	**848.69**	**GalCer (d18:1, h24:1)**
850.68	**850.70**	**GalCer (d18:1, h24:0)**
860.70	860.71	GalCer (d18:1, C26:1)
862.71	862.70	GalCer (d18:1, C26:0)

The neutral GSLs GlcCer and GalCer from human plasma were separated as borate complexes by TLC (see insets of Fig. 2) and isolated by preparative TLC using primulin as nondestructive dye. Monosodiated ions were recorded in the positive ion mode as shown in Fig. 2. Major monohexosylceramides are printed in boldface.

Antibody-detected neutral GSLs

Next, we investigated the GSL extracts from TLC immunostained Lc2Cer, Gb3Cer, Gb4Cer, and nLc4Cer double bands in detail by ESI Q-TOF-MS. The major $[M+Na]^+$ ions identified in the ESI Q-TOF-MS^1 spectra are listed in **Table 3**. Examples of MS^1 spectra including the corresponding insets of anti-Lc2Cer, anti-Gb3Cer, anti-Gb4Cer, and anti-nLc4Cer antibody stained GSLs, where the silica gel bands scraped off the TLC plate are indicated by a dotted rectangle, are provided in **Fig. 4A**, B, C, and D, respectively, for lower-band GSLs of the respective doublets carrying short-chain fatty acids C14 to C18. The main species in the spectra correspond to $[M+Na]^+$ ions of neutral GSLs with saturated C16:0 fatty acids, which may be flanked by the corresponding but low abundant protonated $[M+H]^+$ ions as shown in the Lc2Cer and Gb3Cer spectra in Fig. 4A and B, respectively. In addition to these major species, minor ions indicating GSL species with C14:0 and C18:0 fatty acids were detected as well. None of them, including the dominant C16:0 fatty acid carrying species, showed any modification such as unsaturation or hydroxylation of the acyl chains. The neutral GSLs of the immunostained double bands harboring long-chain C20 to C24 fatty acids are shown in supplementary Fig. I and the major monosodiated ions acquired from the MS^1 spectra are listed in Table 3. As shown for the GSLs with short-chain fatty acids (Fig. 4) no hydroxylated variants were observed in the upper-band spectra of Lc2Cer (supplementary Fig. IA), Gb3Cer (supplementary Fig. IB), Gb4Cer (supplementary Fig. IC), and nLc4Cer (supplementary Fig. ID). Interestingly, GSL heterogeneity owing to variable acylation of the sphingosine (d18:1) moieties with both monounsaturated and saturated C22 to C24 fatty acids was observed for the prevalent tri- and tetrahexosylceramides, whereas Lc2Cer was found to harbor exclusively monounsaturated C24:1 fatty acid.

Stx-detected neutral GSLs

The MS^1 spectra obtained from the silica gel extracts of Stx1/anti-Stx1 and Stx2/anti-Stx2 stained Gb3Cer and Gb4Cer variants were identical to those acquired from the anti-Gb3Cer and anti-Gb4Cer antibody detected species. MS^1 data of Stx1/anti-Stx1 and Stx2/anti-Stx2 detected $[M+Na]^+$ ions are summarized in Table 3 in addition to those obtained by antibody identification. The Stx1 and Stx2 positive TLC overlay assay bands and in particular the monosodiated ions of the MS^1 spectra acquired from the Stx1 stains served as starting point for the final confirmation of Stx-binding Gb3Cer and Gb4Cer species using CID tandem MS. The complete structural characterization was performed for the main species assigned to Gb3Cer and Gb4Cer and is exemplarily shown in the following sections for Gb3Cer and Gb4Cer carrying sphingosine (d18:1) as the sole and constant amino alcohol and a variable fatty

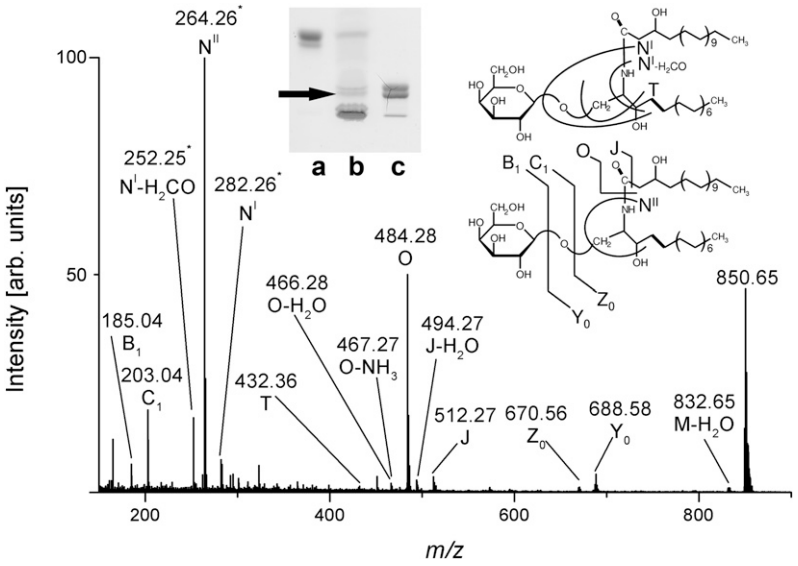

Fig. 3. ESI Q-TOF-MS^2 spectrum of GalCer (d18:1, h24:0) from human plasma. The precursor ions at *m/z* 850.65 were selected from the MS^1 spectrum for CID (see Fig. 2). Fragment ions are assigned with their corresponding *m/z*-values according to the nomenclature introduced by Domon and Costello (61, 62) and Adams and Ann (63). The position of the analyzed GalCer-species is marked with an arrow in the inset, which shows the orcinol stain of a TLC plate. Lane a: Reference GlcCer, 7 μg; lane b: neutral GSL mixture corresponding to 34.7 mg of human plasma protein; lane c: reference GalCer, 10 μg.

acid with chain lengths from C16 to C24 in their ceramide moieties.

Stx-detected Gb3Cer species

The main $[M+Na]^+$ ions detected in the MS^1 spectrum of the positive upper Stx1/anti-Stx1 binding Gb3Cer band (see inset of **Fig. 5A**) correspond to Gb3Cer (d18:1, C24:1/C24:0) at *m/z* 1156.79/1158.79 and Gb3Cer (d18:1, C22:1/C22:0) at *m/z* 1128.75/1130.91 accompanied by low abundant ions at *m/z* 1142.78/1144.78 and *m/z* 1102.87, which could be assigned to Gb3Cer (d18:1, C23:1/C23:0) and Gb3Cer (d18:1, C20:0), respectively, as shown in Fig. 5A.

TABLE 3. Major monosodiated ions identified in the ESI Q-TOF-MS^1 spectra of antibody- and Stx-detected neutral GSLs from human plasma and their proposed structures

$[M+Na]^+$, *m/z* Antibody-Detected	$[M+Na]^+$, *m/z* Stx1-Detected	$[M+Na]^+$, *m/z* Stx2-Detected	Proposed Structure
856.58	n.d	n.d.	Lc2Cer (d18:1, C14:0)
884.59	n.d.	n.d.	Lc2Cer (d18:1, C16:0)
994.68	n.d.	n.d.	Lc2Cer (d18:1, C24:1)
1046.67	1046.67	1046.63	Gb3Cer (d18:1, C16:0)
1074.68	1074.71	1074.64	Gb3Cer (d18:1, C18:0)
1128.74	1128.75	1128.68	Gb3Cer (d18:1, C22:1)
1130.76	1130.91	1130.70	Gb3Cer (d18:1, C22:0)
1142.77	1142.78	1142.75	Gb3Cer (d18:1, C23:1)
1144.77	1144.78	1144.75	Gb3Cer (d18:1, C23:0)
1156.78	1156.79	1156.76	Gb3Cer (d18:1, C24:1)
1158.78	1158.79	1158.77	Gb3Cer (d18:1, C24:0)
1249.73	1249.73	1249.69	Gb4Cer (d18:1, C16:0)
1277.71	1277.80	1277.67	Gb4Cer (d18:1, C18:0)
1331.80	1331.84	1331.94	Gb4Cer (d18:1, C22:1)
1333.86	1333.86	1333.95	Gb4Cer (d18:1, C22:0)
1359.85	1359.85	1359.95	Gb4Cer (d18:1, C24:1)
1361.85	1361.85	1361.99	Gb4Cer (d18:1, C24:0)
1249.77	n.d.	n.d.	nLc4Cer (d18:1, C16:0)
1359.90	n.d.	n.d.	nLc4Cer (d18:1, C24:1)
1361.90	n.d.	n.d.	nLc4Cer (d18:1, C24:0)

Minor protonated $[M+H]^+$ ions detectable in the mass spectra are not listed in the table. Because Stx1 and Stx2 do not bind to Lc2Cer and nLc4Cer, these structures are not detected (n.d.) by both toxins. MS^1 spectra of neutral GSLs with short-chain fatty acids (C14 to C18) are shown in Fig. 4 and those with long-chain fatty acids (C20 to C24) are displayed in supplementary Fig. I.

The complete structural characterization of the Stx1 ligands was exemplified for the main species assigned to Gb3Cer (d18:1, C24:1) by use of low energy CID MS^2 as depicted in Fig. 5B together with the fragmentation scheme in Fig. 5C. The fragment ions originating from the monosodiated precursor ions at *m/z* 1156.75 are assigned according to the nomenclature of Domon and Costello (61, 62) and Adams and Ann (63) and gave rise to the complete structure (**Table 4**). A full series of Y-type ions at *m/z* 994.70 (Y_2), 832.68 (Y_1), and 670.63 (Y_0) was obtained, indicating the sequential loss of three hexose moieties from Gb3Cer and evidencing the Gb3Cer (d18:1, C24:0) structure, which was further supported by the appearance of high abundant B_2 and B_3 as well as C_2 and C_3 ions and additional $^{0,2}A_2$ and $^{0,2}A_3$ ions, the latter two of them generated by ring cleavages (Fig. 5B). The detection of N^{II}-ions at *m/z* 264.29 formed by loss of the N-linked fatty acid of the ceramide moiety and cleavage at the reducing end of the oligosaccharide (Z_0-type ions in addition to Y_0-type ions) clearly indicates the presence of 4-sphingenine (d18:1) and rules out 4-sphinganine (d18:0) as the long-chain aminodiol constituent of the ceramide moiety.

Major $[M+Na]^+$ ions detected at *m/z* 1046.67 in the MS^1 spectrum of the lower Stx1/anti-Stx1 positive band correspond to Gb3Cer (d18:1, C16:0) flanked by low abundant ions at *m/z* 1074.71 assigned to Gb3Cer (d18:1, C18:0) (not shown). The complete structure of Gb3Cer (d18:1, C16:0) was derived by the assignment of fragment ions including diagnostic ions, which were acquired from the monosodiated precursor ions at *m/z* 1046.64 as shown in the CID MS^2 spectrum of the supplementary Fig. IIA and are listed in Table 4.

Stx-detected Gb4Cer species

The prevalent monosodiated molecular ions detected in the MS^1 spectrum of GSL extracts from the upper Stx1/anti-Stx1 binding Gb4Cer band showing a weak positive interaction with the toxin (see inset of **Fig. 6A**) correspond to Gb4Cer (d18:1, C24:1/C24:0) at *m/z* 1359.85/1361.85

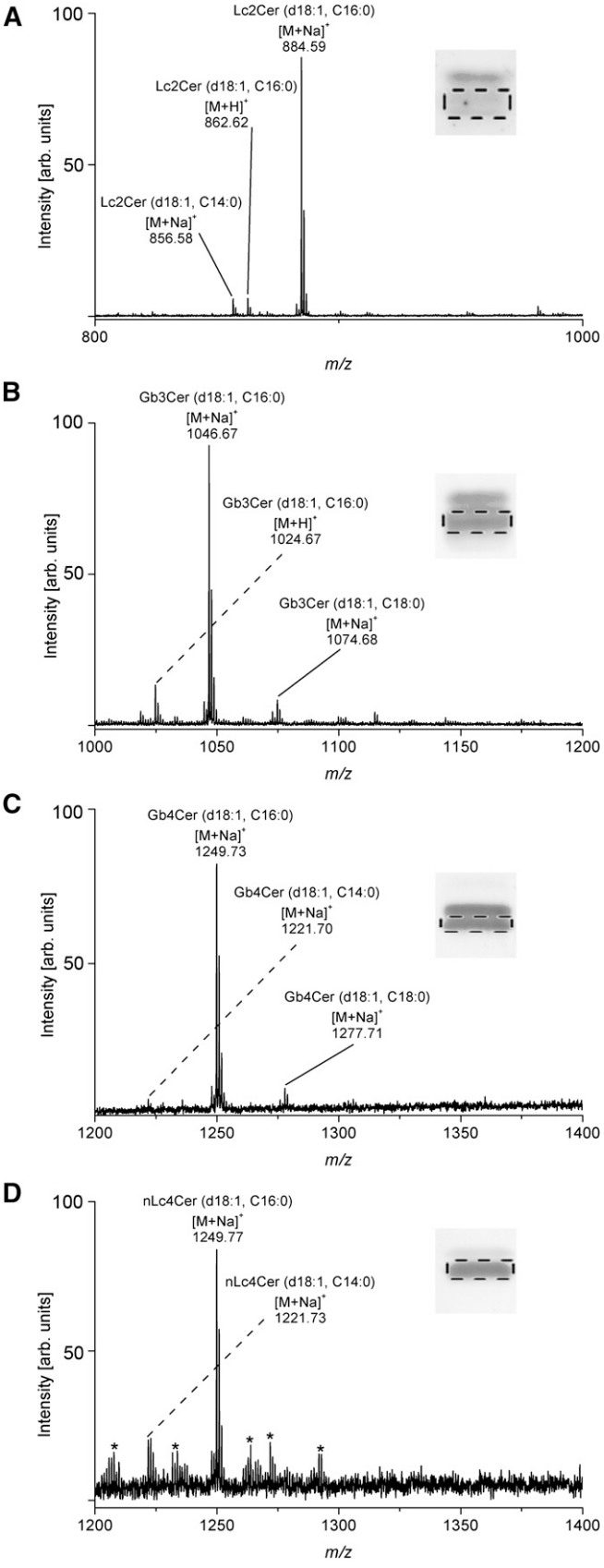

Fig. 4. ESI Q-TOF-MS^1 spectra of immunodetected neutral GSLs with short-chain fatty acids from human plasma. The spectra were acquired from silica gel extracts of antibody-stained GSLs being equivalent to 104.1 mg of human plasma protein, respectively, and recorded in the positive ion mode. The immunostained chromatograms shown in the insets correspond to 17.4 mg of human plasma protein, respectively (see Fig. 1). The dotted frames indicate the lower bands of the respective antibody-detected double bands from which the silica gel extracts were prepared. A: Lc2Cer; B: Gb3Cer; C: Gb4Cer; D: nLc4Cer. ESI Q-TOF-MS^1 spectra of immunodetected neutral GSLs with long-chain fatty acids of the upper bands of the respective antibody-detected double bands are shown in supplementary Fig. I. The major $[M+Na]^+$ ions of the detected neutral GSLs and their proposed structures are listed in Table 3. Unknown ions, which appeared in the spectrum of minor nLc4Cer (D) and originated most likely from the silica gel extraction procedure, are marked with asterisks and were not further analyzed.

and Gb4Cer (d18:1, C22:1/C22:0) at *m/z* 1331.84/1333.86 accompanied by low abundant ions at *m/z* 1345.88/1347.86 assigned to Gb4Cer (d18:1, C23:0) as shown in Fig. 6A. Full structural characterization of these low-affinity Stx1 ligands was performed with the proposed Gb4Cer (d18:1, C24:1) species employing low energy CID MS^2 as demonstrated in Fig. 6B in conjunction with the fragmentation scheme depicted in Fig. 6C. The fragment ions originated from the monosodiated precursor ions at *m/z* 1359.87 exhibited a full series of Y-type ions starting with Y_3 at *m/z* 1156.79, indicating the loss of a HexNAc moiety from the nonreducing end, followed by the sequential cleavage of three hexose moieties, resulting in Y_2 ions at *m/z* 994.72, Y_1 ions at *m/z* 832.68, and ending up with the Y_0 fragment ions at *m/z* 670.62, representing the ceramide moiety carrying C24:1 fatty acid (see synopsis of fragment ions in Table 4). Additionally, a complete series of B-type ions and sporadic C- and Z-type ions were detected, thus enabling, together with the N^{II}-ions at *m/z* 264.27 generated by loss of the N-linked fatty acid of the ceramide moiety and cleavage at the reducing end of the oligosaccharide (Z_0-type ions in addition to Y_0-type ions), an unambiguous structural assignment of Gb4Cer (d18:1, C24:1).

The dominant $[M+Na]^+$ ions detected at *m/z* 1249.73 in the MS^1 spectrum of the GSL extracts of the lower Gb4Cer band with weak Stx1/anti-Stx1 binding capability and the low abundant monosodiated ions at *m/z* 1277.80 were indicative for Gb4Cer (d18:1, C16:0) and Gb4Cer (d18:1, C18:0), respectively (not shown). The proposed structure of Gb4Cer (d18:1, C16:0) could be finally confirmed by CID MS^2 fragmentation and the unequivocal assignment of fragment ions, including diagnostic ions, which were acquired from the monosodiated precursor ions at *m/z* 1249.73. The CID MS^2 spectrum is shown in the supplementary Fig. IIB and fragment ions obtained are summed up in Table 4.

Lipoprotein-associated neutral GSLs

VLDL, LDL, and HDL fractions harboring very low-, low-, and high-density lipoproteins, respectively, were isolated and separated by density gradient ultracentrifugation from the same batch of pooled human plasma, which was used for the structural characterization of individual GSLs from human plasma as described above. Total lipids including GSLs were extracted from lipoprotein fractions and coextracted phospholipids and triglycerides saponified by alkaline treatment. GSL aliquots corresponding to 40 μg of lipoproteins

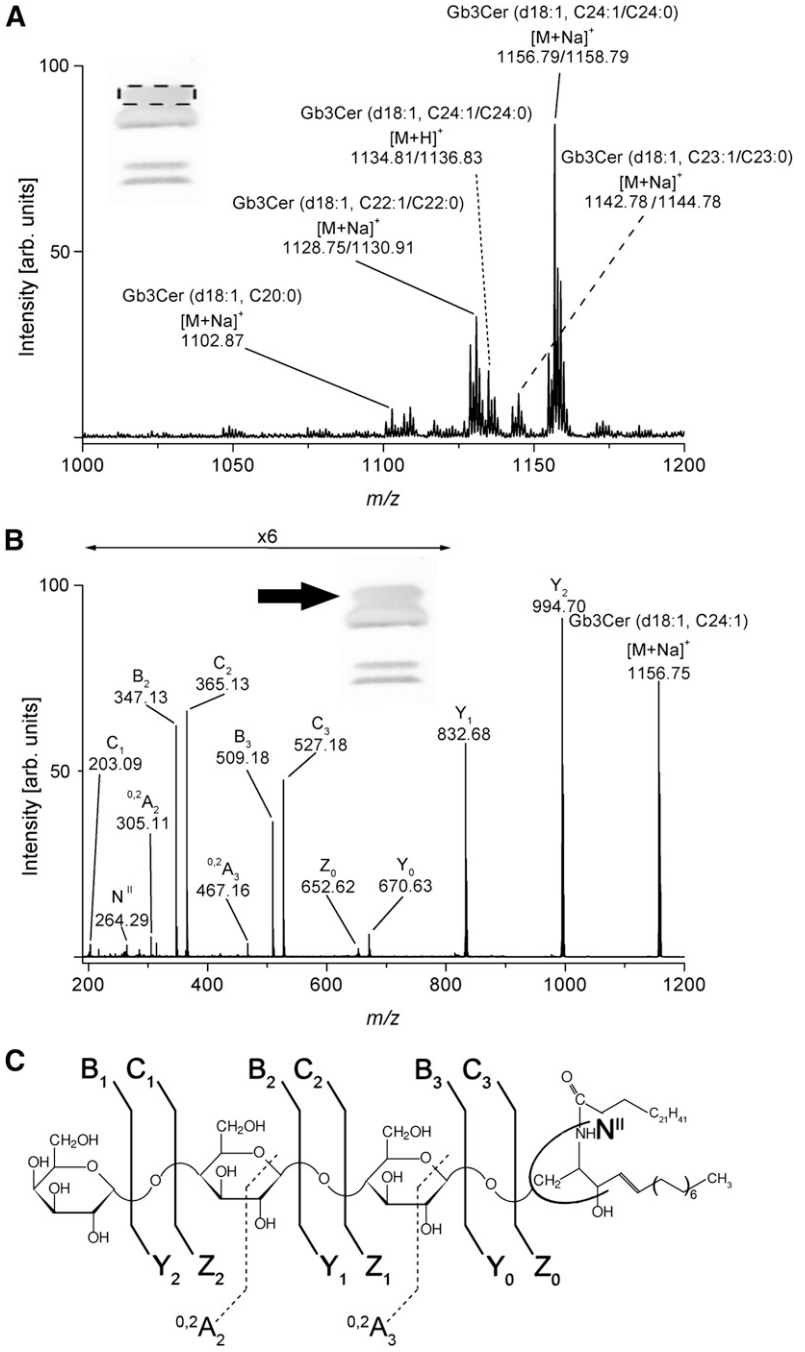

Fig. 5. ESI Q-TOF mass spectra of Stx1-detected Gb3Cer with long-chain fatty acids from human plasma. A: MS^1 spectrum. The spectrum was acquired from a silica gel extract of Stx1/anti-Stx1-antibody detected GSLs being equivalent to 104.1 mg of human plasma protein and recorded in the positive ion mode. The Stx1-stained chromatogram shown in the inset corresponds to 17.4 mg of human plasma protein (see Fig. 1). The dotted frame indicates the upper band of the Stx1-detected Gb3Cer double band from which the silica gel extract was prepared. The major $[M+Na]^+$ ions of Stx1-detected Gb3Cer species and their proposed structures are listed in Table 3. B: MS^2 spectrum of Stx1-bound Gb3Cer (d18:1, C24:1). The Gb3Cer precursor ions at *m/z* 1156.75 were selected from the MS^1 spectrum for CID and fragment ions assigned with their corresponding *m/z*-values. The position of the analyzed Gb3Cer-species is marked with an arrow in the inset. Type of fragment ions and corresponding *m/z*-values are listed in Table 4. C: Fragmentation scheme of Gb3Cer (d18:1, C24:1). The nomenclature introduced by Domon and Costello (61, 62) and Adams and Ann (63) was used for the assignment of the fragment ions.

in case of Lc2Cer and nLc4Cer detection, 60 μg using anti-Gb3Cer and anti-Gb4Cer antibody, and 120 μg employing Stx1 and Stx2 were separated on TLC plates. Neutral GSLs were detected with the same set of anti-GSL antibodies and Stx1 and Stx2 preparations as described above (Table 1). The upper four panels of **Fig. 7** show the TLC immunodetection assays of lipoprotein-associated neutral GSLs with the polyclonal antibodies against Lc2Cer, Gb3Cer, Gb4Cer, and nLc4Cer, and the two lower panels, those TLC overlay assays performed with Stx1/anti-Stx1 and Stx2/anti-Stx2. As being obvious from the antibody assays, all neutral GSLs, which were comparatively analyzed in lipoprotein fractions corresponding to identical protein amounts, preferentially distributed to the VLDL and LDL fractions calculated as percentage values, whereas only low binding intensities could be observed in the HDL fraction (upper four panels of Fig. 7). Stx1 and Stx2 clearly bound to the individual Gb3Cer species showing binding preference to the lower of the two Gb3Cer bands that harbors the Gb3Cer species with the shorter fatty acids, but did not recognize the minute quantities of Gb4Cer species in the lipoprotein fractions, which were also only faintly detectable in the neutral GSL fraction derived from human plasma (lower two panels of Fig. 7). The presence of Gb4Cer, however, could be shown in the lipoprotein fractions and the human plasma sample with the anti-Gb4Cer antibody. Importantly, nonlipoprotein containing fractions, e.g., the intermediate albumin-containing fraction obtained from the ultracentrifugation gradient, did not contain any GSLs, indicating strict association of all neutral GSLs with lipoproteins in human blood.

TABLE 4. Type of fragment ions and corresponding *m/z*-values obtained by ESI Q-TOF-CID-MS^2 of major Stx1-detected Gb3Cer and Gb4Cer species in human plasma

	Gb3Cer		Gb4Cer	
	(d18:1, C16:0) *m/z* 1046.64	(d18:1, C24:1) *m/z* 1156.75	(d18:1, C16:0) *m/z* 1249.73	(d18:1, C24:1) *m/z* 1359.87
Fragment ions	*m/z*-values	*m/z*-values	*m/z*-values	*m/z*-values
$^{0,2}A_2$	305.11	305.11	n.d.	n.d.
$^{0,2}A_3$	467.23	467.16	n.d.	n.d.
B_1; C_1	185.06; 203.07	n.d.; 203.09	226.08; n.d.	226.08; n.d.
B_2; C_2	347.11; 365.13	347.13; 365.13	388.13; n.d.	388.12; n.d.
B_3; C_3	509.15; 527.18	509.18; 527.18	550.18; n.d.	550.17; n.d.
B_4; C_4	n.a.	n.a.	712.25; 730.26	712.25; 730.26
Y_0; Z_0	560.53; 542.52	670.63; 652.62	560.52; n.d.	670.62; 652.61
Y_1; Z_1	722.56; 704.55	832.68; n.d.	722.55; n.d.	832.68; n.d.
Y_2; Z_2	884.62; 866.59	994.70; n.d.	884.62; n.d.	994.72; n.d.
Y_3; Z_3	n.a.	n.a.	1046.68; n.d.	1156.79; n.d.
N^H	264.29	264.29	264.27	264.27

n.a., not applicable; n.d., not detected.

We further evaluated the relative quantitative distribution of neutral GSLs among lipoprotein fractions by TLC scanning densitometry of orcinol-stained bands. Interestingly, Gb3Cer exhibited a similar relative distribution in the lipoprotein fractions compared with human plasma (see supplementary Table I), whereas Lc2Cer was found considerably enriched in the VLDL fraction accompanied by reduced relative content of monohexosylceramides. In addition, a relative decrease of Gb4Cer to half of the plasma value was detected in the VLDL and LDL fractions. This heterogeneity will be addressed in future investigations on the distribution of GSLs within lipoprotein fractions from individual probands.

DISCUSSION

The purpose of this comprehensive study employing MS combined with TLC overlay assay was to explore the molecular diversity of different neutral GSLs from human blood, particularly of those which are supposed to have a functional role in human disease. Mono-, di-, tri-, and tetraosylceramides were exhaustively analyzed by ESI Q-TOF-MS^1 and MS^2 with emphasis on so far unresolved monohexosylceramide composition and neutral GSLs of the globo-series with binding potential to both Stx1 and Stx2.

The monohexosylceramides GlcCer and GalCer were found to constitute approximately one third among the neutral GSLs in human plasma with a relative content of 53% GlcCer and 47% GalCer within the monohexosylceramide fraction. Thus, GalCer represents one of the major neutral GSLs in human plasma that has not been detected (most likely due to failure of separation from GlcCer) in previous investigations (30, 31, 64). For the discrimination of both types of monohexosylceramides, which are indistinguishable using conventional TLC, we reactivated an "old-fashioned" but simple method for separation of GlcCer and GalCer as borate complexes in alkaline solvent, followed by preparative TLC and MS^1 and MS^2 analysis. Their fine characterization by ESI Q-TOF-MS^2 revealed GlcCer species with variable fatty acid chain lengths ranging from C16 to C24 acyl chains. As deduced from the MS^1 spectrum, GlcCer (d18:1, C24:1/C24:0) and GlcCer (d18:1, C22:0) were the most prominent variants. In contrast to this, the fatty acid profile of GalCer ranged from C18 to C26 and ions corresponding to hydroxylated GalCer (d18:1, h24:1/h24:0) showed the highest abundance in the MS^1 spectrum in accordance to the TLC staining intensities. Thus, GalCer with h24:1 and h24:0 acyl chains were the predominant species, whereas only extremely low abundant ions indicative for h24:0 and h24:1 fatty acid appeared in the GlcCer spectrum. Interestingly, the occurrence of GalCer and GalCer-derivatives containing hydroxyl C18 and C24 fatty *N*-acylation is a distinctive feature of vertebrate (including human) myelin from both the central and peripheral nervous system (65, 66, and references therein). Thus, it is tempting to speculate about myelin GalCer as a possible indication of plasma source.

With respect to the development of novel technologies, both GalCer and GlcCer monohexosylceramide molecular species can now be discriminated by ESI MS/MS (67) exploiting the differential fragmentation pattern of GSL using chlorine or Li^+ adducts (68, 69). Furthermore, Zama et al. (70) recently published a novel HPLC-based technology to simultaneously analyze and quantify GalCer and GlcCer using o-phthalaldehyde derivatives prepared with sphingolipid ceramide *N*-deacylase. Due to the biological importance, for example, of GalCer as (co)receptor of HIV-1 gp120 and gp41 (36, 37) or GlcCer exhibiting thrombosis modulatory potential (35) and auxiliary function in Stx-mediated cytotoxicity (34), those techniques might be useful for the determination of GlcCer and GalCer levels in various biological samples such as target tissues or body fluids.

Human serum contains a number of lipid protein complexes that can be isolated on the basis of their different flotation densities and classified as VLDL, LDL, and HDL (38). The protein content of such particles varies from 5% to 60%, and all contain a mixture of neutral lipids, phospholipids, and GSLs organized to form a stable particle. GSLs are present on the surface of all human serum lipoprotein particles where they make up minor constituents

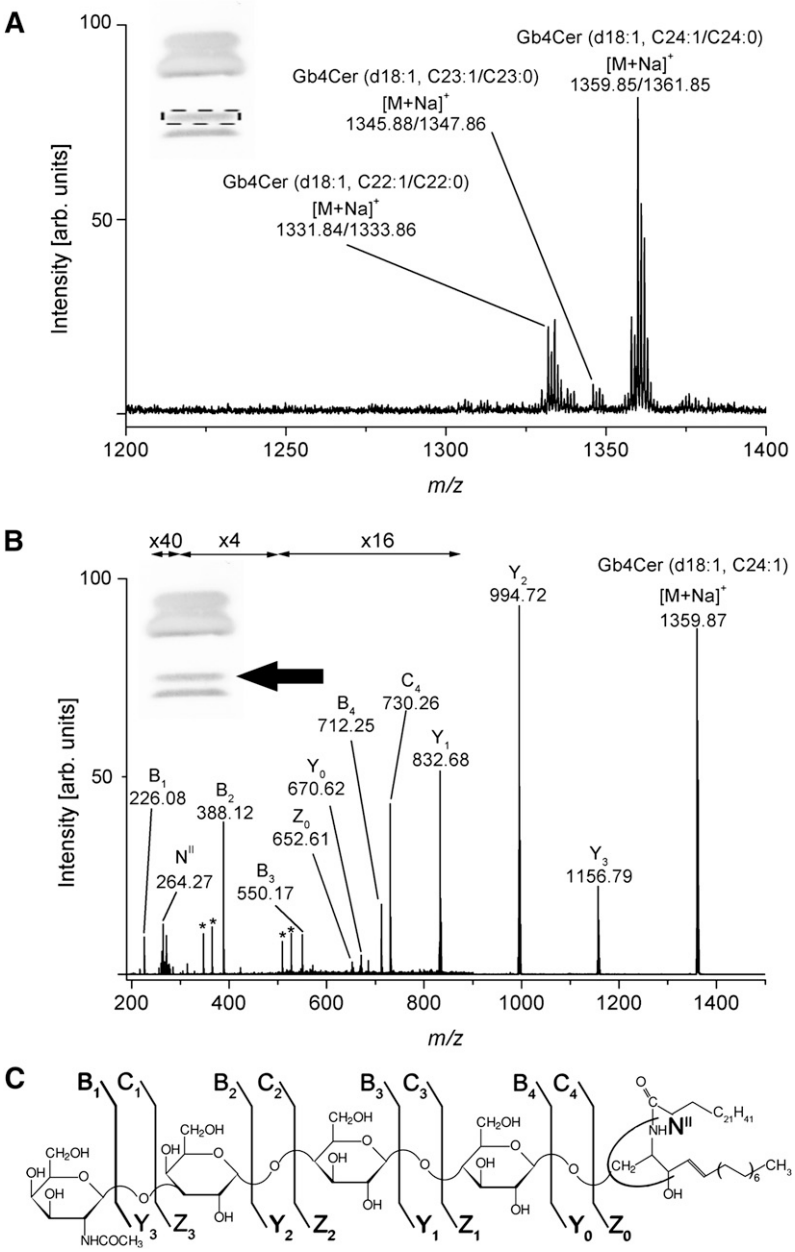

Fig. 6. ESI Q-TOF mass spectra of Stx1-detected Gb4Cer with long-chain fatty acids from human plasma. A: MS^1 spectrum. The spectrum was prepared as described in Fig. 5. The dotted frame indicates the upper band of the Stx1-detected Gb4Cer double band from which the silica gel extract was prepared. The major $[M+Na]^+$ ions of Stx1-detected Gb4Cer species and their proposed structures are listed in Table 3. B: MS^2 spectrum of Stx1-bound Gb4Cer (d18:1, C24:1). The precursor ions at *m/z* 1359.87 were selected from the MS^1 spectrum and the position of the analyzed Gb4Cer-species is marked with an arrow in the inset. Type of fragment ions and corresponding *m/z*-values are listed in Table 4. Asterisks indicate minor fragment ions that originate from internal cleavages of the oligosaccharide. C: Fragmentation scheme of Gb4Cer (d18:1, C24:1). The nomenclature introduced by Domon and Costello (61, 62) and Adams and Ann (63) was used for the assignment of the fragment ions.

in the phospholipid bilayer surrounding the hydrophobic cores of lipoproteins (30). The content of serum lipoprotein fractions may vary depending on the nutritional or hormonal stage of the donors (71) and the GSL content of lipoproteins (so far shown for GlcCer) may increase during infection and inflammation (72, 73). Previous quantitative determination of neutral GSLs revealed 0.6, 0.4, 0.2, and 0.15 μmole/dl in normal human serum for mono-, di-, tri-, and tetraosylceramides, respectively (30). We detected all of the neutral GSLs found in human plasma in each of the three major lipoprotein classes analyzed and no GSLs were detected in the lipoprotein-free fractions obtained by ultracentrifugation. This coincides with several investigations of other research groups, for example, with a study on the GlcCer distribution in human plasma lipoproteins where no GlcCer was detectable in the lipoprotein-deficient plasma (64). Our data revealed predominant presence of GSLs in VLDL and LDL being in some discrepancy with previous quantitative investigations by Dawson et al. (30), who showed roughly similar amounts in VLDL and HDL fractions, whereas considerably lower GSL amounts were detected by us in the HDL fraction. One possible explanation might be that Dawson and colleagues investigated lipoprotein fractions from two Caucasian donors whereas we analyzed lipoproteins from pooled plasma of unknown ethnic origin. Notably, our data were obtained from TLC overlays and expressed on the basis of antibody and Stx staining intensities related to defined milligrams of plasma protein or micrograms of lipoproteins. Direct ESI Q-TOF-MS^1 and MS^2 analysis of the Stx-detected Gb3Cer and Gb4Cer variants demonstrated a broad ceramide heterogeneity of the individual GSL species that ranged from C16 to C24 fatty acid chain length with invariable sphingosine (=4-sphingenine). Furthermore, our study demonstrates almost equal ratios of long-chain C24:1/C24:0 versus short-chain C16:0 fatty acids

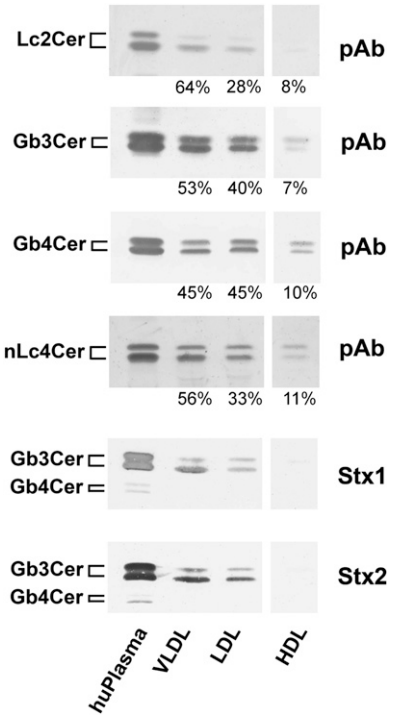

Fig. 7. TLC immunodetection of lipoprotein-associated individual neutral GSLs from human plasma. GSL-aliquots of extracts from VLDL, LDL, and HDL lipoprotein-fractions and from human (hu) plasma were separated by TLC and analyzed with polyclonal antibodies (pAb) against Lc2Cer, Gb3Cer, Gb4Cer, and nLc4Cer in comparison to Stx1/anti-Stx1-antibody and Stx2/anti-Stx2-antibody. Bound anti-GSL and anti-Stx-antibodies were visualized with alkaline phosphatase conjugated secondary antibodies and BCIP as a substrate. Aliquots applied for anti-Lc2Cer and anti-nLc4Cer immunostains correspond to 12.2 mg and those used for anti-Gb3Cer, anti-Gb4Cer, and the Stx1 and Stx2 overlay assays are equivalent to 18.0 mg of human plasma proteins. GSL aliquots of lipoprotein extracts equal the amounts of 40 μg in the anti-Lc2Cer and anti-nLc4Cer, 60 μg in the anti-Gb3Cer and anti-Gb4Cer, and 120 μg of lipoproteins in the Stx1- and Stx2-overlay assays. The densitometrically determined relative distributions of GSLs between the different lipoproteins were calculated as percentage values and are presented for the antibody-detected GSLs as arabic numerals. The vertical white lines indicate areas of noncontiguous lanes assembled. The GSL structures and backgound information on the employed antibodies and Stxs are provided in Table 1.

among the Lc2Cer and globo-series species. The exception was nLc4Cer, which exhibited a preponderance of C16:0 fatty acid in the ceramide portion. Interestingly, hydroxylation as a characteristic feature of the C24:1 and C24:0 fatty acids in the GalCer species did not appear in the Stx-receptors Gb3Cer and Gb4Cer and was found to be restricted to GalCer. This finding is in line with the compositional analysis of GlcCer (the precursor of Lc2Cer, Gb3Cer, and Gb4Cer), indicating almost no hydroxylated C24 acyl chains corresponding to the failure of this modification in Gb3Cer and Gb4Cer. Although GSLs are intimately associated with serum lipoproteins, the mode of association and the implication of fatty acid heterogeneity in this association remain undetermined.

The liver and intestine essentially account for all circulating plasma lipoproteins. Rates of synthesis of lipoproteins from these two organs and their peripheral catabolism determine lipoprotein levels that are normally present in blood (71, 74). Enterocytes, which line the small intestine, assemble chylomicrons from triglycerides, phospholipids, and cholesterol derived from the diet and then secrete the nascent lipoprotein via the lymph into the blood (75) whereas the liver synthesizes and assembles VLDL. Upon secretion, VLDL circulates and its triglyceride core is a substrate for lipoprotein lipase, an enzyme that resides on the luminal surface of the capillary endothelium (71). This leads to the formation of VLDL remnants, which can then be rapidly cleared by the liver or can continue to be processed to become LDL. GSLs are transported in plasma on lipoproteins and are taken up and metabolized by cells through an LDL receptor-mediated pathway. However, only sparse data are available about the biological and functional role of lipoprotein-associated GSLs. A few early studies have evidenced the reversible exchange of GSLs between HDL and LDL (76) and, moreover, that cholera toxin insensitive cells can acquire a functional cholera toxin receptor ganglioside GM1 following culture in the presence of serum lipoproteins (77). Due to the strict association of Gb3Cer with lipoproteins in human blood, it is tempting to speculate on the functional role of lipoprotein-associated Gb3Cer in human blood as transporter of Stx from the intestine into the circulation. We thus speculate that this way, Stx might reach the microvascular endothelial cells of the kidney and the brain, which represent the major targets of Stx in the clinical onset of HUS.

Thus, despite the hypothetical functional role of GSLs, our study provides useful information for future investigations of the transfer of neutral GSLs among lipoproteins and from lipoproteins to cells. Furthermore, the analysis of the molecular details of Stx-receptors and their association with lipoproteins in patients suffering from Stx-mediated diseases such as HUS may help us to better understand the involvement of GSLs in the interaction with Stxs and to inspire us to develop preventive and therapeutic measures for Stx-mediated diseases (78).

The authors thank Dr. Martina Bielaszewska and Dr. Iris Meisen (Institute for Hygiene, University of Münster) for providing Shiga toxins for the TLC overlay assays and help with quantitative scanning densitometry, respectively. The expert technical assistance of Nadine Brandt is gratefully acknowledged.

REFERENCES

1. Levery, S. B. 2005. Glycosphingolipid structural analysis and glycosphingolipidomics. *Methods Enzymol.* **405:** 300–369.
2. Müthing, J., and U. Distler. 2010. Advances on the compositional analysis of glycosphingolipids combining thin-layer chromatography with mass spectrometry. *Mass Spectrom. Rev.* **29:** 425–479.
3. Pruett, S. T., A. Bushnev, K. Hagedorn, M. Adiga, C. A. Haynes, M. C. Sullards, D. C. Liotta, and A. H. Merrill, Jr. 2008. Biodiversity of sphingoid bases ("sphingosines") and related amino alcohols. *J. Lipid Res.* **49:** 1621–1639.
4. Merrill, A. H., Jr., T. H. Stokes, A. Momin, H. Park, B. J. Portz, S. Kelly, E. Wang, M. C. Sullards, and M. D. Wang. 2009. Sphingolipidomics;

a valuable tool to understanding the roles of sphingolipids in biology and disease. *J. Lipid Res.* **50:** S97–S102.
5. Sonnino, S., A. Prinetti, L. Mauri, V. Chigorno, and G. Tettamanti. 2006. Dynamic and structural properties of sphingolipids as driving forces for the formation of membrane domains. *Chem. Rev.* **106:** 2111–2125.
6. Pike, L. J. 2009. The challenge of lipid rafts. *J. Lipid Res.* **50:** S323–S328.
7. Ledeen, R. W., and G. Wu. 2008. Nuclear sphingolipids: metabolism and signalling. *J. Lipid Res.* **49:** 1176–1186.
8. Lopez, P. H., and R. L. Schnaar. 2009. Gangliosides in cell recognition and membrane protein regulation. *Curr. Opin. Struct. Biol.* **19:** 549–557.
9. Ariga, T., M. P. McDonald, and R. K. Yu. 2008. Role of ganglioside metabolism in the pathogenesis of Alzheimer's disease–a review. *J. Lipid Res.* **49:** 1157–1175.
10. Yu, R. K., Y. Nakatami, and M. Yanagisawa, M. 2009. The role of glycosphingolipid metabolism in the developing brain. *J. Lipid Res.* **50:** S440–S445.
11. Karlsson, K. A. 1989. Animal glycosphingolipids as membrane attachment sites for bacteria. *Annu. Rev. Biochem.* **58:** 309–350.
12. Smith, D. C., J. M. Lord, L. M. Roberts, and L. Johannes. 2004. Glycosphingolipids as toxin receptors. *Semin. Cell Dev. Biol.* **15:** 397–408.
13. Müthing, J., C. H. Schweppe, H. Karch, and A. W. Friedrich. 2009. Shiga toxins, glycosphingolipid diversity, and endothelial cell injury. *Thromb. Haemost.* **101:** 252–264.
14. Sandvig, K. 2001. Shiga toxins. *Toxicon.* **39:** 1629–1635.
15. Karch, H., P. I. Tarr, and M. Bielaszewska. 2005. Enterohaemorrhagic *Escherichia coli* in human medicine. *Int. J. Med. Microbiol.* **295:** 405–418.
16. Ling, H., A. Boodhoo, B. Hazes, M. D. Cummings, G. D. Armstrong, J. L. Brunton, and R. J. Read. 1998. Structure of the Shiga-like toxin I B-pentamer complexed with an analogue of its receptor Gb_3. *Biochemistry.* **37:** 1777–1788.
17. Bielaszewska, M., and H. Karch. 2005. Consequences of enterohaemorrhagic *Escherichia coli* infection for the vascular endothelium. *Thromb. Haemost.* **94:** 312–318.
18. Sandvig, K., Ø. Garred, K. Prydz, J. V. Kozlov, S. H. Hansen, and B. van Deurs. 1992. Retrograde transport of endocytosed Shiga toxin to the endoplasmic reticulum. *Nature.* **358:** 510–512.
19. Endo, Y., K. Tsurugi, T. Yutsudo, Y. Takeda, T. Ogasawara, and K. Igarashi. 1988. Site of action of a Vero toxin (VT2) from *Escherichia coli* O157:H7 and Shiga toxin on eukaryotic ribosomes. *Eur. J. Biochem.* **171:** 45–50.
20. Garred, Ø., B. van Deurs, and K. Sandvig. 1995. Furin-induced cleavage and activation of Shiga toxin. *J. Biol. Chem.* **270:** 10817–10821.
21. Proulx, F., E. G. Seidman, and D. Karpman. 2001. Pathogenesis of Shiga toxin-associated hemolytic uremic syndrome. *Pediatr. Res.* **50:** 163–171.
22. Tarr, P. I., C. A. Gordon, and W. L. Chandler. 2005. Shiga-toxin-producing *Escherichia coli* and haemolytic uraemic syndrome. *Lancet.* **365:** 1073–1086.
23. Ståhl, A. L., L. Sartz, A. Nelsson, Z. D. Békássy, and D. Karpman. 2009. Shiga toxin and lipopolysaccharide induce platelet-leukocyte aggregates and tissue factor release, a thrombotic mechanism in haemolytic uremic syndrome. *PLoS One.* **4:** e6990.
24. Hurley, B. P., C. M. Thorpe, and D. W. Acheson. 2001. Shiga toxin translocation across intestinal epithelial cells is enhanced by neutrophil transmigration. *Infect. Immun.* **69:** 6148–6155.
25. Holgersson, J., P. Å. Jovall, and M. E. Breimer. 1991. Glycosphingolipids of human large intestine: detailed structural characterization with special reference to blood group compounds and bacterial receptor structures. *J. Biochem.* **110:** 120–131.
26. Brigotti, M., A. Caprioli, A. E. Tozzi, P. L. Tazzari, F. Ricci, R. Conte, D. Carnicelli, M. A. Procaccino, F. Minelli, A. V. S. Ferretti, et al. 2006. Shiga toxins present in the gut and in the polymorphonuclear leukocytes circulating in the blood of children with hemolytic-uremic syndrome. *J. Clin. Microbiol.* **44:** 313–317.
27. Brigotti, M., D. Carnicelli, E. Ravanelli, S. Barbieri, F. Ricci, A. Bontadini, A. E. Tozzi, G. Scavia, A. Caprioloi, and P. L. Tazzari. 2008. Interactions between Shiga toxins and human polymorphonuclear leukocytes. *J. Leukoc. Biol.* **84:** 1019–1027.
28. Chatterjee, S., and P. O. Kwiterovich, Jr. 1984. Glycosphingolipids and plasma lipoproteins: a review. *Can. J. Biochem. Cell Biol.* **62:** 385–397.
29. Lingwood, C. A. 1996. Role of verotoxin receptors in pathogenesis. *Trends Microbiol.* **4:** 147–153.
30. Dawson, G., A. W. Kruski, and A. M. Scanu. 1976. Distribution of glycosphingolipids in the serum lipoproteins of normal human subjects and patients with hypo- and hyperlipidemias. *J. Lipid Res.* **17:** 125–131.
31. Kundu, S. K., I. Diego, S. Osovitz, and D. M. Marcus. 1985. Glycosphingolipids of human plasma. *Arch. Biochem. Biophys.* **238:** 388–400.
32. Schiller, J., O. Zschörnig, M. Petković, M. Müller, J. Arnhold, and K. Arnold. 2001. Lipid analysis of human HDL and LDL by MALDI-TOF mass spectrometry and ^{31}P-NMR. *J. Lipid Res.* **42:** 1501–1508.
33. Sommer, U., H. Herscovitz, F. K. Welty, and C. E. Costello. 2006. LC-MS-based method for qualitative and quantitative analysis of complex lipid mixtures. *J. Lipid Res.* **47:** 804–814.
34. Smith, D. C., D. J. Sillence, T. Falguières, R. M. Jarvis, L. Johannes, J. M. Lord, F. M. Platt, and L. M. Roberts. 2006. The association of Shiga-like toxin with detergent-resistant membranes is modulated by glucosylceramide and is an essential requirement in the endoplasmic reticulum for a cytotoxic effect. *Mol. Biol. Cell.* **17:** 1375–1387.
35. Deguchi, H., J. A. Fernández, I. Pabinger, J. A. Heit, and J. H. Griffin. 2001. Plasma glucosylceramide deficiency as potential risk factor for venous thrombosis and modulator of anticoagulant protein C pathway. *Blood.* **97:** 1907–1914.
36. Fantini, J., D. G. Cook, N. Nathanson, S. L. Spitalnik, and F. Gonzalez-Scarano. 1993. Infection of colonic epithelial cell lines by type 1 human immunodeficiency virus is associated with cell surface expression of galactosylceramide, a potential alternative gp120 receptor. *Proc. Natl. Acad. Sci. USA.* **90:** 2700–2704.
37. Alfsen, A., and M. Bomsel. 2002. HIV-1 gp41 envelope residues 650–685 exposed native virus act as a lectin to bind epithelial cell galactosyl ceramide. *J. Biol. Chem.* **277:** 25649–25659.
38. Havel, R. J., H. A. Eder, and J. H. Bragdon. 1955. The distribution and chemical composition of ultracentrifugally separated lipoproteins in human serum. *J. Clin. Invest.* **34:** 1345–1353.
39. Lowry, O. H., N. J. Rosebrough, A. L. Farr, and R. J. Randall. 1951. Protein measurement with the Folin phenol reagent. *J. Biol. Chem.* **193:** 265–275.
40. Ledeen, R. W., and R. K. Yu. 1982. Gangliosides: structure, isolation, and analysis. *Methods Enzymol.* **83:** 139–191.
41. Müthing, J., H. Egge, B. Kniep, and P. F. Mühlradt. 1987. Structural characterization of gangliosides from murine T lymphocytes. *Eur. J. Biochem.* **163:** 407–416.
42. Müthing, J., U. Maurer, K. Šoštarić, U. Neumann, H. Brandt, S. Duvar, J. Peter-Katalinić, and S. Weber-Schürholz. 1994. Differential distribution of glycosphingolipids in mouse rabbit skeletal muscle demonstrated by biochemical and immunohistological analyses. *J. Biochem.* **115:** 64–73.
43. Smith, H. W., and M. A. Linggood. 1971. The transmissible nature of enterotoxin production in a human enteropathogenic strain of *Escherichia coli*. *J. Med. Microbiol.* **4:** 301–305.
44. Strockbine, N. A., L. R. M. Marques, J. W. Newland, H. W. Smith, R. K. Holmes, and A. D. O'Brien. 1986. Two toxin-converting phages from *Escherichia coli* O157:H7 strain 933 encode antigenically distinct toxins with similar biologic activities. *Infect. Immun.* **53:** 135–140.
45. Petric, M., M. A. Karmali, S. Richardson, and R. Cheung. 1987. Purification and biological properties of *Escherichia coli* verotoxin. *FEMS Microbiol. Lett.* **41:** 63–68.
46. Head, S. C., M. A. Karmali, and C. A. Lingwood. 1991. Preparation of VT1 and VT2 hybrid toxins from their purified dissociated subunits. *J. Biol. Chem.* **226:** 3617–3621.
47. Kasai, M., M. Iwamori, Y. Nagai, K. Okumura, and T. Tada. 1980. A glycolipid on the surface of mouse natural killer cells. *Eur. J. Immunol.* **10:** 175–180.
48. Chester, M. A. 1999. IUPAC-IUB Joint Commission on Biochemical Nomenclature. Nomenclature of glycolipids. Recommendations 1997. *Glycoconj. J.* **16:** 1–6.
49. Saito, T., and S. I. Hakomori. 1971. Quantitative isolation of total glycosphingolipids from animal cells. *J. Lipid Res.* **12:** 257–259.
50. Meisen, I., A. W. Friedrich, H. Karch, U. Witting, J. Peter-Katalinić, and J. Müthing. 2005. Application of combined high-performance thin-layer chromatography immunostaining and nanoelectrospray ionisation quadrupole time-of-flight tandem mass spectrometry to the structural characterization of high- and low-affinity binding ligands of Shiga toxin 1. *Rapid Commun. Mass Spectrom.* **19:** 3659–3665.
51. Duvar, S., J. Peter-Katalinić, F. G. Hanisch, and J. Müthing. 1997. Isolation and structural characterization of glycosphingolipids of

in vitro propagated bovine aortic endothelial cells. *Glycobiology.* **7:** 1099–1109.
52. Kean, E. L. 1966. Separation of gluco- and galactocerebrosides by means of borate thin-layer chromatography. *J. Lipid Res.* **7:** 449–452.
53. Skipski, V. P. 1975. Thin-layer chromatography of neutral glycosphingolipids. *Methods Enzymol.* **35:** 396–425.
54. Meisen, I., J. Peter-Katalinić, and J. Müthing. 2004. Direct analysis of silica gel extracts from immunostained glycosphingolipids by nanoelectrospray ionization quadrupole time-of-flight mass spectrometry. *Anal. Chem.* **76:** 2248–2255.
55. Müthing, J. 1998. TLC in structure and recognition studies of glycosphingolipids. *In* Methods in Molecular Biology. E. F. Hounsell, editor. Humana Press Inc., Totawa, NJ. 183–195.
56. Müthing, J., S. Duvar, D. Heitmann, F. G. Hanisch, U. Neumann, G. Lochnit, R. Geyer, and J. Peter-Katalinić. 1999. Isolation and structural characterization of glycosphingolipids of *in vitro* propagated human umbilical vein endothelial cells. *Glycobiology.* **9:** 459–468.
57. Distler, U., M. Hülsewig, J. Souady, K. Dreisewerd, J. Haier, N. Senninger, A. W. Friedrich, H. Karch, F. Hillenkamp, S. Berkenkamp, et al. 2008. Matching IR-MALDI-o-TOF mass spectrometry with the TLC overlay binding assay and its clinical application for tracing tumor-associated glycosphingolipids in hepatocellular and pancreatic cancer. *Anal. Chem.* **80:** 1835–1846.
58. Schweppe, C. H., M. Bielaszewska, G. Pohlentz, A. W. Friedrich, H. Büntemeyer, M. A. Schmidt, K. S. Kim, J. Peter-Katalinić, H. Karch, and J. Müthing. 2008. Glycosphingolipids in vascular endothelial cells: relationship of heterogeneity in Gb3Cer/CD77 receptor expression with differential Shiga toxin 1 cytotoxicity. *Glycoconj. J.* **25:** 291–304.
59. Distler, U., J. Souady, M. Hülsewig, I. Drmić-Hofman, J. Haier, A. W. Friedrich, H. Karch, N. Senninger, K. Dreisewerd, S. Berkenkamp, et al. 2009. Shiga toxin receptor Gb3Cer/CD77: tumor association and promising therapeutic target in pancreas and colon cancer. *PLoS One.* **4:** e6813.
60. Meisen, I., J. Peter-Katalinić, and J. Müthing. 2003. Discrimination of neolacto-series gangliosides with α2–3- and α2–6-linked *N*-acetylneuraminic acid by nanoelectrospray ionization low-energy collision-induced dissociation tandem quadrupole TOF MS. *Anal. Chem.* **75:** 5719–5725.
61. Domon, B., and C. E. Costello. 1988. A systematic nomenclature for carbohydrate fragmentations in FAB-MS/MS spectra of glycoconjugates. *Glycoconj. J.* **5:** 397–409.
62. Domon, B., and C. E. Costello. 1988. Structure elucidation of glycosphingolipids and gangliosides using high-performance tandem mass spectrometry. *Biochemistry.* **27:** 1534–1543.
63. Adams, J., and Q. Ann. 1993. Structure determination of sphingolipids by mass spectrometry. *Mass Spectrom. Rev.* **12:** 51–85.
64. Chatterjee, S., W. R. Bell, and P. O. Kwiterovich, Jr. 1984. Distribution of antithrombin III and glucosylceramide in human plasma lipoproteins and lipoprotein deficient plasma. *Lipids.* **19:** 363–366.
65. Dasgupta, S., S. B. Levery, and E. L. Hogan. 2002. 3-*O*-acetyl-sphingosine series myelin glycolipids: characterization of novel 3-*O*-acetyl-sphingosine galactosylceramide. *J. Lipid Res.* **43:** 751–761.
66. Bennion, B., S. Dasgupta, E. L. Hogan, and S. B. Levery. 2007. Characterization of novel myelin components 3-*O*-acetyl-sphingosine galactosylceramides by electrospray ionization Q-TOF MS and MS/CID-MS of Li^+ adducts. *J. Mass Spectrom.* **42:** 598–620.
67. Shaner, R. L., J. C. Allegood, H. Park, E. Wang, S. Kelly, C. A. Haynes, M. C. Sullards, and A. H. Merrill, Jr. 2009. Quantitative analysis of sphingolipids for lipidomics using triple quadrupole and quadrupole linear ion trap mass spectrometers. *J. Lipid Res.* **50:** 1692–1707.
68. Han, X., and H. Cheng. 2005. Characterization and direct quantitation of cerebroside molecular species from lipid extracts by shotgun lipidomics. *J. Lipid Res.* **46:** 163–175.
69. Bennion, B., S. Dasgupta, E. L. Hogan, and S. B. Levery. 2007. Characterization of novel myelin components 3-*O*-acetyl-sphingosine galactosylceramides by electrospray ionization Q-TOF MS and MS/CID-MS of Li^+ adducts. *J. Mass Spectrom.* **42:** 598–620.
70. Zama, K., Y. Hayashi, S. Ito, Y. Hirabayashi, T. Inoue, K. Ohno, N. Okino, and M. Ito. 2009. Simultaneous quantification of glucosylceramide and galactosylceramide by normal-phase HPLC using *O*-phthalaldehyde derivatives prepared with sphingolipid ceramide *N*-deacylase. *Glycobiology.* **19:** 767–775.
71. Blasiole, D. A., R. A. Davis, and A. D. Attie. 2007. The physiological and molecular regulation of lipoprotein assembly and secretion. *Mol. Biosyst.* **3:** 608–619.
72. Memon, R. A., W. M. Holleran, A. H. Moser, T. Seki, Y. Uchida, J. Fuller, J. K. Shigenaga, C. Grunfeld, and K. R. Feingold. 1998. Endotoxin and cytokines increase hepatic sphingolipid biosynthesis and produces lipoproteins enriched in ceramides and sphingomyelin. *Arterioscler. Thromb. Vasc. Biol.* **18:** 1257–1265.
73. Khovidhunkit, W., M. S. Kim, R. A. Memon, J. K. Shigenaga, A. H. Moser, K. R. Feingold, and C. Grunfeld. 2004. Effects of infection and inflammation on lipid and lipoprotein metabolism: mechanisms and consequences to the host. *J. Lipid Res.* **45:** 1169–1196.
74. Field, F. J., and S. N. Mathur. 1995. Intestinal lipoprotein synthesis and secretion. *Prog. Lipid Res.* **34:** 185–198.
75. Hoofnagle, A. N., and J. W. Heinecke. 2009. Lipoproteomics: using mass spectrometry-based proteomics to explore the assembly, structure, and function of lipoproteins. *J. Lipid Res.* **50:** 1967–1975.
76. Loeb, J. A., and G. Dawson. 1982. Reversible exchange of glycosphingolipids between human high and low density lipoproteins. *J. Biol. Chem.* **257:** 11982–11987.
77. Fishman, P. H., R. M. Bradley, J. Moss, and V. C. Manganiello. 1978. Effect of serum on ganglioside uptake and choleragen responsiveness of transformed mouse fibroblasts. *J. Lipid Res.* **19:** 77–81.
78. Karmali, M. A. 2004. Prospects for preventing serious systemic toxemic complications of Shiga toxin producing *Escherichia coli* infections using Shiga toxin receptor analogues. *J. Infect. Dis.* **189:** 355–359.